An adaptive filtered-*x* algorithm for energy-based active control

Scott D. Sommerfeldt and Peter J. Nashif[a)]
Applied Research Laboratory and Graduate Program in Acoustics, The Pennsylvania State University, P.O. Box 30, State College, Pennsylvania 16804

(Received 22 July 1993; revised 13 January 1994; accepted 1 April 1994)

A control algorithm based on the filtered-*x* LMS algorithm is developed that has the property of being able to control the energy in the acoustic field. The algorithm is useful for providing greater global control of the field than is obtained by controlling the pressure. This is due to the fact that the energy-based approach effectively overcomes the observability problems that often limit the performance possible when controlling the pressure field. The control approach is developed for the cases of a predominantly standing wave field, and a predominantly propagating wave field. The approach is applicable for both broadband and narrow-band excitations. A simple example demonstrating the increased performance possible with the energy-based control approach is presented for the case of single frequency excitation.

PACS numbers: 43.40.Vn

INTRODUCTION

A number of different techniques and control algorithms have received considerable attention recently for active control of sound and vibration fields. With regards to the active control of sound fields, there have been significant gains made in a theoretical understanding of the mechanisms of active control, and the interaction between the primary excitation sources and the secondary control sources.[1,2]

Along with the theoretical developments, there has also been significant progress made in implementing practical active control systems. A number of different control algorithms have been developed for active control. However, the active control systems reported in the literature have relied most prominently on the filtered-*x* algorithm[3,4] or the recursive least-mean-squares algorithm.[5] These algorithms have the property of being relatively simple to implement, as well as being rather robust.

Another issue related to active control that has received considerable attention recently is that of the optimal location for the sensors and actuators used. The importance of this issue can be seen intuitively by considering a standing wave field. If the sensor or actuator is placed at a node of the standing wave, there will be an observability or controllability problem, respectively. However, it should be noted that the optimal location for the sensors and actuators is a function of the desired control objective. Thus a related question that deserves critical attention is exactly what the desired control objective is and what the appropriate performance function is to achieve that objective.

The effect of choosing a different performance function has been investigated by Curtis *et al.*[6] In their work, they considered the difference between minimizing the total power output of the primary and secondary sources, which represents a "global" performance function, and maximizing the power absorption of each secondary source, which represents a "local" performance function. This comparison represents a difficulty often encountered in practice, in that one often wishes to control a global variable, such as the total acoustic potential energy in an enclosure or the total power output of a source array, while only having local information available, such as discrete pressure measurements. Thus an important question is often whether a suitable local performance function can be found that at least approximates the global control of the field that is desired.

In applications of active control to acoustic fields, the measurement that is typically most readily available is pressure. However, for most applications, the control objective that is desired is often related to the energy in the field, rather than the pressure associated with the field. Several examples include the control of the sound field in a duct, where one typically wishes to minimize the acoustic intensity that propagates past the secondary control source, and the control of the sound field in an enclosure, where one often wishes to minimize the global potential energy in the enclosure. In both of these applications, the approach that has usually been taken is to measure the acoustic pressure at a discrete number of locations and to minimize the sum of the squared pressures. The reasoning for this approach is that the intensity that propagates in a duct is proportional to the squared pressure and the potential energy in an enclosure is found as the spatial integral of the squared pressure. However, it has been found that one must be careful in using this approach in practice. In the case of sound propagation in a duct, there are evanescent higher-order modes that can degrade the control of the acoustic intensity that is obtained if the error sensor is positioned too close to the secondary control source.[7] Also, standing waves that may result from a reflective termination in the duct can easily distort the equivalence of squared pressure and acoustic intensity. In the case of enclosed sound fields, modal coupling exists, such that minimizing the squared pressure may result in "control spillover," whereby controlling the pressure at the discrete error sensors results in energy being coupled into other modes, resulting in a global potential energy that may actually increase in some cases. These difficulties result from the fact that the effect of using a number of discrete error sensors is to produce an observability problem, in that the sensors can only sense a subset of the modes contributing to the acoustic field.

In an attempt to overcome some of the difficulties of

[a)]Current address: Ford Electronics, 19540 Allen Road, Melvindale, MI 48122.

 0001-4966/94/96(1)/300/7/$6.00

trying to achieve global control by controlling only local pressure measurements, a control approach has been developed that allows one to monitor and control the energy in the field, rather than a single acoustic parameter such as pressure. The control approach has the distinct advantage that it generally gives a better approximation to the desired global control, since it is inherently associated with the control of energy, rather than a single scalar acoustic parameter. While the method will be outlined here for acoustic fields, it is also directly applicable to controlling structural vibration fields, and has been so used in other applications.[8]

I. DEVELOPMENT OF ENERGY-BASED CONTROL

The method of energy-based control utilizes the concept of controlling a local variable in an attempt to achieve global control, but the local variable chosen is an energy-based quantity. In general, there are two cases of interest. In the first case, the acoustic field to be controlled is predominantly composed of energy in the form of standing waves, such as the sound field in enclosures. For this case, the energy-based quantity chosen consists of the sum of the potential and kinetic energy densities at discrete locations. The reason for this choice is related to the concept that a standing wave field can be described in terms of modes, which are typically coupled for acoustic fields. By controlling the total energy density, the observability problem that leads to performance degradation when using discrete pressure measurements is overcome. This is due to the fact that if the magnitude of the potential energy density associated with a particular mode goes to zero at an error sensor location, the kinetic energy density will approach a maximum. Thus all modes of the enclosure are observable by controlling the energy density, since the method is sensitive to both the pressure and velocity associated with the mode.

For the second case, the acoustic field to be controlled consists of propagating energy, such as the sound field in a duct or free-field propagation. For this case, the energy-based quantity to control is the acoustic intensity. The acoustic intensity has the advantage of being sensitive to the propagating energy without being sensitive to the nonpropagating energy associated with the evanescent modes of the duct or the near field of a source.

A. Development of the control law

The control law for controlling the energy density in an acoustic standing wave field will be fully developed in this section, from which it is straightforward to modify the results for the case of controlling acoustic intensity. In addition, the algorithm will be developed here for a single control source and a single error sensor, for simplicity. The method can be readily extended to multiple sources and error sensors using the method outlined by Elliott *et al.*[4]

The acoustic energy density at an arbitrary location in the field is given by

$$w=p^2/2\rho c^2+\tfrac{1}{2}\rho v^2, \tag{1}$$

where ρ is the ambient fluid density, c is the acoustic phase speed, p is the acoustic pressure, and v is the acoustic particle velocity. The acoustic pressure and velocity are both

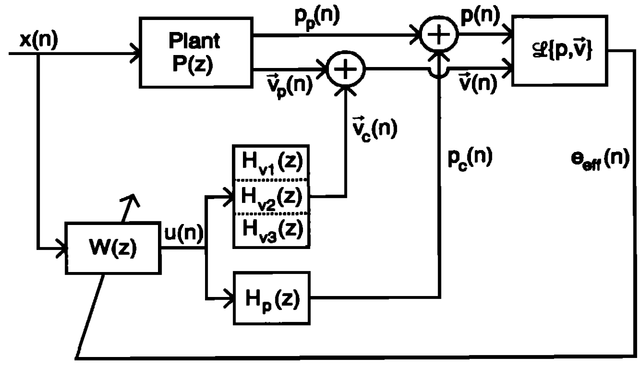

FIG. 1. Block diagram representation of a filtered-x control implementation for controlling acoustic energy density.

composed of two components: the pressure or velocity due to the primary excitation source(s), and the pressure or velocity due to the secondary control source(s).

A filtered-x control implementation for this case can be represented in block diagram form as shown in Fig. 1. In this figure, $p_p(n)$ and $\vec{v}_p(n)$ represent the pressure and particle velocity at the error sensor location in the absence of any control, while $p_c(n)$ and $\vec{v}_c(n)$ are the pressure and particle velocity at the error sensor due to control. It should be noted that n represents a discrete-time index. Here, $\mathbf{W(z)}$ represents the transfer function of the adaptive control filter, while $\mathbf{H_{v1}(z)}$, $\mathbf{H_{v2}(z)}$, $\mathbf{H_{v3}(z)}$, and $\mathbf{H_p(z)}$ represent the transfer functions relating the control output $u(n)$ to the velocity components and pressure at the error sensor that result from the control source. Finally, $\mathscr{L}\{p,\vec{v}\}$ represents any processing of the pressure and velocity signals that occurs to obtain the "effective" error signal. In a standard filtered-x implementation, this operator would simply be equal to unity.

To proceed with the derivation of the energy-based algorithm, the pressure and velocity components at the error sensor can be represented as

$$v_1(n)=v_{1p}(n)+\sum_{j=0}^{J-1} h_{v1j}(n)u(n-j), \tag{2a}$$

$$v_2(n)=v_{2p}(n)+\sum_{j=0}^{J-1} h_{v2j}(n)u(n-j), \tag{2b}$$

$$v_3(n)=v_{3p}(n)+\sum_{j=0}^{J-1} h_{v3j}(n)u(n-j), \tag{2c}$$

$$p(n)=p_p(n)+\sum_{k=0}^{K-1} h_{pk}(n)u(n-k), \tag{3}$$

where h_{v1j}, h_{v2j}, h_{v3j}, and h_{pk} represent the coefficients of $\mathbf{H_{v1}(z)}$, $\mathbf{H_{v2}(z)}$, $\mathbf{H_{v3}(z)}$, and $\mathbf{H_p(z)}$, and a finite impulse response (FIR) structure has been assumed for the transfer functions. One could also use an infinite impulse response (IIR) implementation for these transfer functions if desired. In addition, for the velocity components, the subscript 1 refers to the x direction, the subscript 2 to the y direction, and the subscript 3 to the z direction. For a filtered-x implementation, the control output $u(n)$ is given by

$$u(n)=\sum_{i=0}^{I-1} w_i(n)x(n-i), \tag{4}$$

where $x(n)$ is a reference input signal, chosen to be correlated with the signal to be controlled. Substituting this expression into Eqs. (2) and (3) yields

$$v1(n)=v_{1p}(n)+\sum_{i=0}^{I-1} w_i(n)\sum_{j=0}^{J-1} h_{v1j}(n)x(n-j-i), \tag{5a}$$

$$v2(n)=v_{2p}(n)+\sum_{i=0}^{I-1} w_i(n)\sum_{j=0}^{J-1} h_{v2j}(n)x(n-j-i), \tag{5b}$$

$$v3(n)=v_{3p}(n)+\sum_{i=0}^{I-1} w_i(n)\sum_{j=0}^{J-1} h_{v3j}(n)x(n-j-i), \tag{5c}$$

$$p(n)=p_p(n)+\sum_{i=0}^{I-1} w_i(n)\sum_{k=0}^{K-1} h_{pk}(n)x(n-k-i). \tag{6}$$

In Eqs. (5) and (6), the order of the summations has been interchanged, which is permissible if one assumes the coefficients $w_i(n)$ to be time-invariant. Physically, this assumption corresponds to the assumption that the filtered-x coefficients vary slowly, relative to the time scale of the response of the system to be controlled. From Eqs. (5) and (6), it is possible to define

$$r_{v1}(n-i)=\sum_{j=0}^{J-1} h_{v1j}(n)x(n-j-i), \tag{7a}$$

$$r_{v2}(n-i)=\sum_{j=0}^{J-1} h_{v2j}(n)x(n-j-i), \tag{7b}$$

$$r_{v3}(n-i)=\sum_{j=0}^{J-1} h_{v3j}(n)x(n-j-i), \tag{7c}$$

$$r_p(n-i)=\sum_{k=0}^{K-1} h_{pk}(n)x(n-k-i), \tag{8}$$

which can be referred to as "filtered-x" signals. It is also useful to define the following vector quantities:

$$\mathbf{W}^{\mathbf{T}}(n)=[w_0(n)w_1(n)\cdots w_{I-1}(n)], \tag{9}$$

$$\mathbf{R}_{\mathbf{v1}}^{\mathbf{T}}(n)=[r_{v1}(n)r_{v1}(n-1)\cdots r_{v1}(n-I+1)], \tag{10a}$$

$$\mathbf{R}_{\mathbf{v2}}^{\mathbf{T}}(n)=[r_{v2}(n)r_{v2}(n-1)\cdots r_{v2}(n-I+1)], \tag{10b}$$

$$\mathbf{R}_{\mathbf{v3}}^{\mathbf{T}}(n)=[r_{v3}(n)r_{v3}(n-1)\cdots r_{v3}(n-I+1)], \tag{10c}$$

$$\mathbf{R}_{\mathbf{p}}^{\mathbf{T}}(n)=[r_p(n)r_p(n-1)\cdots r_p(n-I+1)]. \tag{11}$$

Using vector notation allows Eqs. (5) and (6) to be expressed as

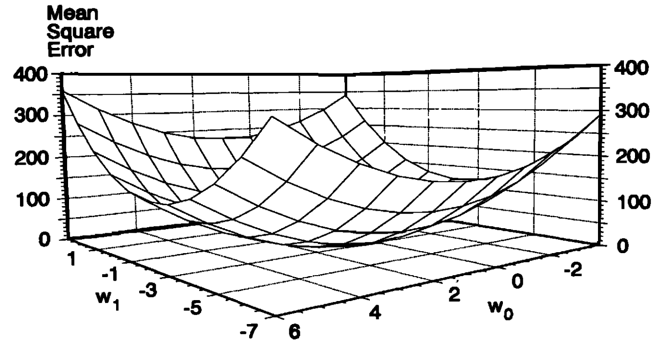

FIG. 2. Performance function error surface for two control filter coefficients. The optimum filter coefficients in this example are $(w_0,w_1)=(1.2,-2.3)$ and the minimum mean-square-error is given by 0.05.

$$v_1(n)=v_{1p}(n)+\mathbf{W}^{\mathbf{T}}(n)\mathbf{R}_{\mathbf{v1}}(n), \tag{12a}$$

$$v_2(n)=v_{2p}(n)+\mathbf{W}^{\mathbf{T}}(n)\mathbf{R}_{\mathbf{v2}}(n), \tag{12b}$$

$$v_3(n)=v_{3p}(n)+\mathbf{W}^{\mathbf{T}}(n)\mathbf{R}_{\mathbf{v3}}(n), \tag{12c}$$

$$p(n)=p_p(n)+\mathbf{W}^{\mathbf{T}}(n)\mathbf{R}_{\mathbf{p}}(n). \tag{13}$$

To proceed, it is useful to consider the standard development of the filtered-x algorithm. The filtered-x algorithm is based on a least-mean-squares (LMS) approach, such that the performance function to be minimized is chosen to be a positive definite quadratic function of the filter coefficients. Since the performance function is quadratic with respect to the filter coefficients, this function can be represented as a hyperparabolic surface in an $(I+1)$-dimensional space, where I represents the number of filter coefficients used. An example of this function for two filter coefficients can be seen in Fig. 2. One major advantage of an LMS approach is that one is guaranteed to have a unique global minimum for the performance function that is being minimized. For an acoustic field, the pressure at some location in the field is a linear function of the control filter coefficients, as can be seen from Eq. (13). Thus a typical filtered-x implementation uses the squared pressure at one or more discrete locations as the performance function that is to be minimized. As such, the pressure at the sensor location is referred to as the "error" signal, the squared pressure is used for the performance function, and the filter coefficients are updated in real-time according to the negative gradient of the performance function, which leads to the standard result,[3]

$$\mathbf{W}(n+1)=\mathbf{W}(n)-\mu e(n)\mathbf{R}_{\mathbf{p}}(n). \tag{14}$$

Here, μ is a convergence parameter chosen to maintain stability, $e(n)$ is the measured pressure at the sensor location, and $\mathbf{R}_{\mathbf{p}}(n)$ is as defined in Eqs. (8) and (11).

B. Energy density control update

To develop the control law for controlling the acoustic energy density, one might consider using the squared energy density as the performance function to minimize, analogous to using the squared pressure for a typical implementation. However, from Eq. (1) it can be seen that the squared energy density is fourth-order in the acoustic pressure and velocity.

Since the pressure and velocity are both linear functions of the filter coefficients, this choice of performance function does not lead to a single, unique, global minimum. Thus, for controlling the acoustic energy density, the appropriate performance function to minimize to obtain a filtered-x implementation is the energy density itself. As can be seen from Eqs. (1), (12), and (13), the energy density is a positive definite quadratic function of the filter coefficients, thus yielding a single, unique, global minimum when the function is minimized. It can also be noted that by choosing the acoustic energy density as the performance function, one can think of the square root of the energy density as being the "effective error" signal. While this may not have much physical meaning, this effective error signal is analogous to the pressure error signal in typical implementations.

Choosing the acoustic energy density as the performance function allows the performance function to be expressed as

$$J_{ed}=\sum_{m=1}^{3}\frac{1}{2}\rho[v_{mp}(n)+\mathbf{W}^{\mathrm{T}}(n)\mathbf{R}_{\mathbf{vm}}(n)]^2+\frac{1}{2\rho c^2}[p_p(n)+\mathbf{W}^{\mathrm{T}}(n)\mathbf{R}_{\mathbf{p}}(n)]^2, \tag{15}$$

where use has been made of Eqs. (12) and (13). To update the control filter coefficients, the gradient of the performance function is needed. This can be obtained as

$$\begin{aligned}\nabla J_{ed}&=\sum_{m=1}^{3}\rho[v_{mp}(n)+\mathbf{W}^{\mathrm{T}}(n)\mathbf{R}_{\mathbf{vm}}(n)]\mathbf{R}_{\mathbf{vm}}(n)\\&\quad+\frac{1}{\rho c^2}[p_p(n)+\mathbf{W}^{\mathrm{T}}(n)\mathbf{R}_{\mathbf{p}}(n)]\mathbf{R}_{\mathbf{p}}(n)\\&=\sum_{m=1}^{3}\rho v_m(n)\mathbf{R}_{\mathbf{vm}}(n)+\frac{1}{\rho c^2}p(n)\mathbf{R}_{\mathbf{p}}(n).\end{aligned} \tag{16}$$

Thus the implementation of the control law can be expressed as

$$\mathbf{W}(n+1)=\mathbf{W}(n)-\mu\left(\sum_{m=1}^{3}\rho v_m(n)\mathbf{R}_{\mathbf{vm}}(n)+\frac{1}{\rho c^2}p(n)\mathbf{R}_{\mathbf{p}}(n)\right). \tag{17}$$

To implement the control law in this form requires measurements of the acoustic pressure and velocity at the error sensor location, as well as a measure of the transfer functions designated as $\mathbf{H}_{\mathbf{vm}}(\mathbf{z})$ and $\mathbf{H}_{\mathbf{p}}(\mathbf{z})$ in Fig. 1, which are required to determine $\mathbf{R}_{\mathbf{vm}}(n)$ and $\mathbf{R}_{\mathbf{p}}(n)$. These transfer functions can be estimated either *a priori* or in real time using one of several available adaptive methods.[9–11] The acoustic velocity could be obtained using a particle velocity sensor, such as a laser vibrometer or velocity microphone, or using a two-microphone technique, such as is typically used to measure acoustic intensity. In general, three orthogonal velocity measurements will be required to estimate the velocity vector. If the two sensor approach is used, Eq. (17) can be written in a slightly different form. For this case, the pressure and velocity (x component) are expressed as

$$p(n)\approx\frac{p_1(n)+p_2(n)}{2}, \tag{18}$$

$$v_1(n)\approx\frac{-1}{\rho\Delta x}\int[p_2(n)-p_1(n)]dn, \tag{19}$$

where $p_1(n)$ and $p_2(n)$ are the pressure measurements from the two closely spaced microphones, and Δx is the spacing between them. Similar expressions exist for the y and z components of the velocity. These expressions can be simplified somewhat by defining

$$p_{\mathrm{avg}}(n)=\frac{p_1(n)+p_2(n)}{2}, \tag{20}$$

$$\gamma_1(n)=\int[p_2(n)-p_1(n)]dn. \tag{21}$$

Using these expressions in Eq. (17) allows the update equation for the two-microphone method to be expressed as

$$\mathbf{W}(n+1)=\mathbf{W}(n)-\mu\left(\frac{p_{\mathrm{avg}}(n)}{\rho c^2}\mathbf{R}_{\mathbf{p}}(n)-\sum_{m=1}^{3}\frac{\gamma_m(n)}{\Delta x_m}\mathbf{R}_{\mathbf{vm}}(n)\right). \tag{22}$$

The previous update expressions [Eqs. (17) and (22)] are exact, but require the knowledge of all the transfer functions, $\mathbf{H}_{\mathbf{vm}}(\mathbf{z})$ and $\mathbf{H}_{\mathbf{p}}(\mathbf{z})$, which relate the control filter output $u(n)$ to the velocity and pressure at the error sensor location. Under certain conditions, it is possible to simplify the update equation so that knowledge of only $\mathbf{H}_{\mathbf{p}}(\mathbf{z})$ is required. This simplifies the implementation of the algorithm, but in general will not be exact, as one assumption is introduced.

Euler's equation can be used to relate $\mathbf{R}_{\mathbf{vm}}(\mathbf{n})$ to $\mathbf{R}_{\mathbf{p}}(\mathbf{n})$ as

$$\mathbf{R}_{\mathbf{vm}}(n)=\frac{-1}{\rho}\int\nabla_m\mathbf{R}_{\mathbf{p}}(n)dn, \tag{23}$$

where ∇_m indicates the component of the gradient in the direction indicated by m. Using Eq. (23) in Eq. (16) allows the gradient of the performance function to be expressed as

$$\nabla J_{ed}=\sum_{m=1}^{3}\left(-v_m(n)\int\nabla_m\mathbf{R}_{\mathbf{p}}(n)dn\right)+\frac{p(n)}{\rho c^2}\mathbf{R}_{\mathbf{p}}(n). \tag{24}$$

Several possibilities exist for dealing with the gradient and integral operators in Eq. (24). The approach used here assumes that the space-time dependence of the wave field is such that the effect of the integral and gradient operators is such as to yield a factor of $1/c$. This assumption neglects a possible phase shift, and as such may not be valid in some cases. Using this assumption allows Eq. (24) to be expressed as

$$\nabla J_{ed}\approx\frac{\mathbf{R}_{\mathbf{p}}(n)}{\rho c}\left(\frac{p(n)}{c}-\sum_{m=1}^{3}\rho v_m(n)\right). \tag{25}$$

Using Eq. (25) allows the control update equation to be expressed as

$$\mathbf{W}(n+1)=\mathbf{W}(n)-\mu\left(\frac{p(n)}{c}-\sum_{m=1}^{3}\rho v_m(n)\right)\mathbf{R}(n), \tag{26}$$

where $\mathbf{R}(n)=\mathbf{R}_\mathbf{p}(n)/\rho c$. If a two-microphone method is implemented, Eq. (26) can be expressed as

$$\mathbf{W}(n+1)=\mathbf{W}(n)-\mu\left(\frac{p_{\text{avg}}(n)}{c}+\sum_{m=1}^{3}\frac{\gamma_m(n)}{\Delta x_m}\right)\mathbf{R}(n). \tag{27}$$

C. Acoustic intensity control update

To implement energy-based control for acoustic intensity, the instantaneous acoustic intensity in a chosen direction is selected as the performance function, since it is quadratic in the control filter coefficients. Thus the "effective error" signal is the square root of the instantaneous acoustic intensity. It should be noted, however, that this choice of performance function can lead to potential difficulties, since the acoustic intensity is not a positive definite function in general. As a result, using the negative gradient of the quadratic performance function can yield an unstable solution if one is not careful. As an example, consider the case in which the acoustic intensity in minimized at a location lying between the primary source and the control source. If the intensity component to be minimized is along the line between the sources, the intensity will be positive from one of the sources, and will be negative from the other source. As a result, the solution that minimizes the acoustic intensity for this case will be for the control source to have either zero source strength or maximum source strength, depending on whether the acoustic sensor is located in the positive or negative direction from the control source. Therefore, the appropriateness of implementing this approach is restricted to cases where the geometry is such that the intensity component to be minimized will have the same sign for both sources. If this assumption holds, the performance function will be positive definite, and a unique minimum will exist.

A second option for controlling acoustic intensity would be to minimize the square of the intensity. This approach guarantees that the performance function will be positive definite, as desired, but introduces the problem of having a nonquadratic function. The result is that multiple minima may occur, and one must be able to determine whether the minimum that the algorithm converges to is a local or global minimum. In this paper, it is assumed that the geometry of the control problem can be arranged so that the acoustic intensity is positive definite and serves as a suitable performance function.

Using Eqs. (12) and (13) allows the intensity performance function to be expressed as

$$J_{\text{int}}=p(n)v(n)=[p_p(n)+\mathbf{W}^\mathbf{T}(n)\mathbf{R}_\mathbf{p}(n)]\times[v_p(n)+\mathbf{W}^\mathbf{T}(n)\mathbf{R}_v(n)], \tag{28}$$

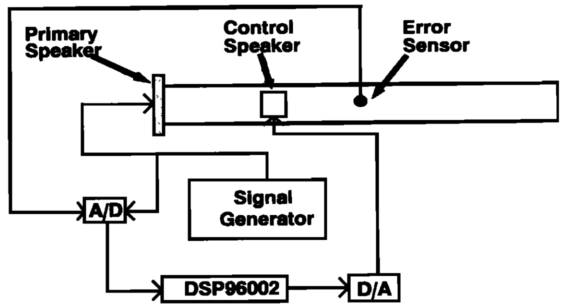

FIG. 3. Schematic of the experimental configuration.

where the subscripts have been dropped from the velocity terms, since only a single component is being considered. Taking the gradient of the performance function yields

$$\nabla J_{\text{int}}=p(n)\mathbf{R}_v(n)+v(n)\mathbf{R}_\mathbf{p}(n), \tag{29}$$

and the control update equation can be expressed as

$$\mathbf{W}(n+1)=\mathbf{W}(n)-\mu[p(n)\mathbf{R}_v(n)+v(n)\mathbf{R}_\mathbf{p}(n)]. \tag{30}$$

As for the case of controlling energy density, this expression can be modified to account for using a two-microphone method or to express $\mathbf{R}_v(n)$ in terms of $\mathbf{R}_p(n)$.

It is of interest to note that if only plane waves exist, then $v(n)=p(n)/\rho c$ and $\mathbf{R}_v(n)=\mathbf{R}_p(n)/\rho c$. For this case, Eq. (30) reduces to

$$\mathbf{W}(n+1)=\mathbf{W}(n)-\mu p(n)\mathbf{R}(n), \tag{31}$$

where $\mathbf{R}(n)=2\mathbf{R}_p(n)/\rho c$. Equation (31) represents the filtered-x control law that has been found to work very well in controlling acoustic propagation in ducts when the error sensor is located a sufficient distance away from the sources so that evanescent wave effects are negligible. Implementing the more general expression in Eq. (30) is more involved, but offers the capability of accounting for near-field effects if evanescent waves are present.

II. EXAMPLE

This section presents an example of energy-based control to provide some indication of the performance that can be expected. The example chosen corresponds to controlling the acoustic energy density in an enclosure. For simplicity, a one-dimensional sound field is considered, which is obtained by using a closed circular duct of length 5.6 m and diameter 0.116 m as shown in Fig. 3. The uncontrolled acoustic field is generated by a loudspeaker positioned at one end of the duct, driven at a frequency of 200 Hz. A single loudspeaker control source is arbitrarily located at a normalized position of $0.34L$, where L is the length of the duct, and a single error sensor is located at a position of $0.47L$. The error sensor consists of two calibrated and phase-matched microphones with a spacing between them of 1.7 cm. It is of note that the sensor position is near the center of the duct, where half of the modes for the enclosure have a pressure minimum. Thus one would expect this to be a poor location, in general, for trying to control the sound field by minimizing the pressure at the error sensor.

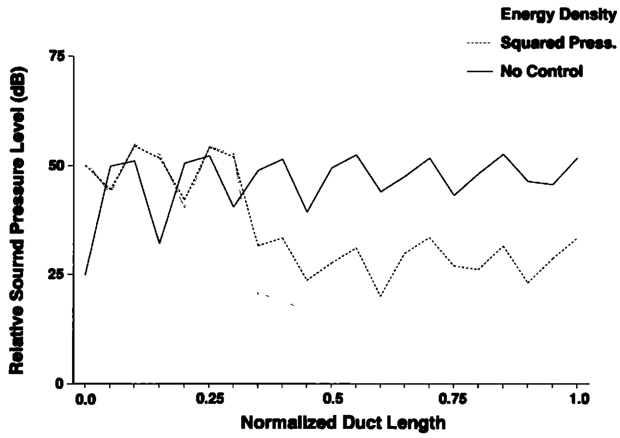

FIG. 4. Predicted sound-pressure level along the duct for an excitation frequency of 200 Hz and different control implementations.

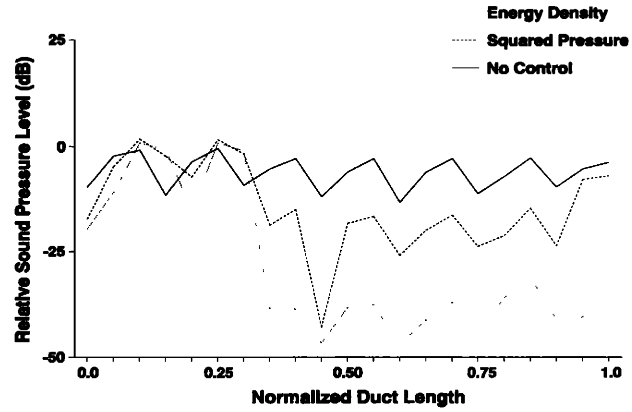

FIG. 5. Measured sound-pressure level along the duct for an excitation frequency of 200 Hz and different control implementations.

Controlling the acoustic field was investigated both numerically and experimentally. The numerical results were determined using a modal description of the field, in which the lowest 50 modes were considered. It was verified that 50 modes were adequate to describe the field in the frequency range of interest. For a given source/sensor configuration, the optimal control source strength was calculated to minimize the chosen performance function. The pressure throughout the enclosure was then calculated, both with and without control.

As a means of comparison, both control of the acoustic pressure at the error sensor and control of the acoustic energy density at the error sensor are considered. The control equation used for controlling the energy density is given in Eq. (27). The subtraction and integration required to obtain $\gamma(n)$ was accomplished by means of an analog circuit consisting of a differential amplifier, integrator, and amplifier. For this application, the analog integrator was designed to provide accurate integration above approximately 125 Hz. The gain of the circuit and the spacing between the two microphones were measured and used in the control software, along with a nominal value for c of 343 m/s, to maintain the same relative gain on each of the terms in Eq. (27).

Figure 4 shows the predicted numerical results, while Fig. 5 shows the corresponding measured experimental results for the cases of no control, controlling the pressure, and controlling the energy density. For these results, there is a single-frequency excitation at 200 Hz, which corresponds to an off-resonance frequency that lies approximately halfway between the sixth and seventh modes of the enclosure. As can be seen, there is good agreement between the numerical and experimental results. Both methods indicate very substantial attenuation in the vicinity of the error sensor ($x = 0.47L$). It should be noted that for these results, the pressure was measured at 21 uniformly spaced locations along the enclosure. The error sensor location was not at one of these locations, and so is not included in the results of Fig. 5. However, the pressure was reduced the greatest at the error sensor, and would produce an even sharper notch for the squared pressure curve in Fig. 5 if that data point was included. It is apparent from Fig. 5 that throughout most of the enclosure, controlling the energy density gives considerably improved attenuation over controlling the acoustic pressure. For the region between the primary source and the control source, neither method attenuates the acoustic field significantly, although the method of controlling energy density tends to give slightly improved results in this region. This result is a function of the source configuration, and could be improved by optimizing the control source location. Further results and considerably more discussion of controlling the acoustic energy density in this enclosure can be found in Refs. 12 and 13.

III. ISSUES ASSOCIATED WITH ENERGY-BASED CONTROL

There are several advantages and disadvantages associated with energy-based control that should be addressed. It is apparent that more signal processing is required to implement energy-based control than acoustic-pressure based control, since a direct measurement from the error sensor is not sufficient for updating the control filter coefficients. [Compare Eqs. (14) and (17), for example.] However, with the current digital signal processing hardware available, the difference in signal processing required is often a fairly insignificant issue, unless a large number of control filters is envisioned. For example, if the simplified algorithm of Eq. (27) can be used, only two additional multiplications (using the inverse of division) and one addition is required for each control filter used. If the control law in Eq. (17) is implemented, the additional computations for each control filter is given by $N+2$ multiplications and 1 addition, where N is the number of coefficients in each control filter.

Another issue associated with energy-based control is that typically two highly phase-matched microphones are required to obtain energy quantities if a two-microphone method is used, which can imply a relatively high cost for the sensors. However, several manufacturers offer low cost microphones that are sufficiently stable so that one can find two reasonably well phased-matched microphones without too much difficulty. In addition, since one is interested in controlling the energy, rather than in mapping the field, one can tolerate some error in the energy estimate. This can be seen by considering the energy density expression in Eq. (1). If one considers a pure standing wave field, the kinetic energy density will be equal to the potential energy density in magnitude. Thus a perfect sensor would weight the two terms equally. The effect of errors in the pressure and velocity estimates is to weight one of the energy density terms more than the other. However, the control system will still be sensitive to all modes associated with the field since both kinetic and potential energy densities are being monitored. In fact, one of the major advantages of energy-based control is that it minimizes observability problems associated with the modes of the field, and this advantage is not negated by small measurement errors that slightly affect the weighting of the terms.

Another issue of interest is that a pressure-based error signal only requires a single sensor for each error signal, while an energy-based error signal requires multiple sensors for an acoustic field. Thus the question might be asked if controlling energy density with a single "energy density sensor" (two microphones, for example) performs any better than simply controlling the pressure at two discrete error sensor locations. Controlling the pressure at several locations still makes it possible to have control spillover problems, as all modes that have a small pressure amplitude at the sensor locations can be excited to high amplitudes without being sensed by the control system. However, this cannot occur when controlling the energy density, since the high velocity amplitude at the pressure minima would be detected by the "energy density sensor" as part of the kinetic energy density term, and hence would be controlled. In fact, there is some indication that using energy-density control may actually reduce the total number of transducers required to achieve global control of an acoustic field.[14]

One final issue to address with energy-based control is that of the optimal error sensor location. The performance obtained when controlling acoustic pressure is generally a strong function of the error sensor location. For example, if the sensor is placed near a pressure node, poor performance can be expected. However, the energy density in a standing wave field or the acoustic intensity associated with a propagating wave does not demonstrate any such dependence on sensor location. Thus another significant advantage of energy-based control is that the control method is relatively insensitive to the error sensor location. (The same is not true for the control source location.) As a result, placement of the error sensors is not a critical issue when using energy-based control, which can be very advantageous in applications where practical considerations limit the possible locations for the sensors.

IV. SUMMARY

An energy-based active control scheme has been developed that can be implemented to control acoustic or structural fields. Since the control approach is based on the concept of monitoring and controlling energy quantities, it is generally capable of achieving greater global control of the acoustic field, since it is sensitive to the energy in the field, rather than the pressure at a point. Methods have been presented that are appropriate for controlling either standing wave or propagating wave fields.

By sensing the energy in the field, the method has the advantage of overcoming the observability problem that often leads to localized zones of silence when controlling the measured pressure in a field. In addition, the energy quantities that are monitored do not have the strong spatial dependence that the pressure field typically has, so that the problem of optimizing the error sensor location(s) is minimized. The convergence properties associated with this control scheme are similar to those associated with a standard filtered-x implementation, and only a modest increase in signal processing is required to implement the energy-based control scheme.

[1] S. J. Elliott, P. Joseph, P. A. Nelson, and M. E. Johnson, "Power output minimization and power absorption in the active control of sound," J. Acoust. Soc. Am. **90**, 2501–2512 (1991).

[2] S. D. Snyder and C. H. Hansen, "Active noise control in ducts: Some physical insights," J. Acoust. Soc. Am. **86**, 184–194 (1989).

[3] B. Widrow and S. D. Stearns, *Adaptive Signal Processing* (Prentice-Hall, Englewood Cliffs, NJ, 1985), pp. 288–294.

[4] S. J. Elliott, I. M. Stothers, and P. A. Nelson, "A multiple error LMS algorithm and its application to the active control of sound and vibration," IEEE Trans. Acoust. Speech, Sig. Process. **ASSP-35**, 1423–1434 (1987).

[5] L. J. Eriksson, M. C. Allie, and R. A. Greiner, "The selection and application of an IIR adaptive filter for use in active sound attenuation," IEEE Trans. Acoust. Speech Sig. Process. **ASSP-35**, 433–437 (1987).

[6] A. R. D. Curtis, P. A. Nelson, and S. J. Elliott, "Active reduction of a one-dimensional enclosed sound field: An experimental investigation of three control strategies," J. Acoust. Soc. Am. **88**, 2265–2268.

[7] J. Tichy, G. E. Warnaka, and L. A. Poole, "A study of active control of noise in ducts," J. Vib. Acoust. Stress Reliab. Design, **106**, 399–404 (1984).

[8] A. E. Schwenk, S. D. Sommerfeldt, and S. I. Hayek, "Adaptive control of structural intensity associated with bending waves in a beam," J. Acoust. Soc. Am. (accepted for publication).

[9] S. D. Sommerfeldt and J. Tichy, "Adaptive control of a two-stage vibration isolation mount," J. Acoust. Soc. Am. **88**, 938–944 (1990).

[10] S. D. Sommerfeldt, "Multi-channel adaptive control of structural vibration," Noise Control Eng. J. **37**, 77–89 (1991).

[11] L. J. Eriksson, "Development of the filtered-*U* algorithm for active noise control," J. Acoust. Soc. Am. **89**, 257–265 (1991).

[12] P. Nashif, "An energy-density-based control strategy for minimizing the sound field in enclosures," M. S. thesis, The Pennsylvania State University, University Park, PA (1992).

[13] S. D. Sommerfeldt and P. J. Nashif, "Energy based control of the sound field in enclosures," in *Proceedings of the Second International Congress on Recent Developments in Vibration* (Mechanical Engineering Dept., Auburn University, 1992), pp. 361–368.

[14] S. D. Sommerfeldt and P. J. Nashif, "A comparison of control strategies for minimizing the sound field in enclosures," Proc. Noise-Con 91, 299–306 (July 1991).